Densities of degeneracies and near-degeneracies

Michael Wilkinson and Elizabeth J. Austin
Department of Physics and Applied Physics, John Anderson Building, University of Strathclyde, Glasgow G4 ONG, Scotland, United Kingdom
(Received 7 July 1992)

The eigenvalues of a quantum system depending on two parameters become degenerate at isolated points in the parameter space, which are called diabolical points because of their double-cone structure. Varying one parameter produces near-degeneracies termed avoided crossings. Some results on the density of these objects in parameter space can be obtained by requiring consistency with the level repulsion exhibited by the distribution of energy-level spacings. The density of diabolical points and the distribution of their ellipticities are obtained exactly for the Gaussian orthogonal ensemble random-matrix model. The distribution of their separations in parameter space is also investigated.

PACS number(s): 03.65.Sq, 05.45.+b

I. INTRODUCTION

It is well known that if the energy levels of a quantum system with a discrete spectrum are plotted as a function of a parameter, the curves for levels of the same symmetry class do not cross. The curves can, however, approach each other at events called "avoided crossings," where the separation of the energy levels becomes small compared to the mean level spacing: the energy-level curves have a universal structure in the neighborhood of an avoided crossing which can be determined from degenerate perturbation theory. If we consider the energy levels of a system (which we assume has time-reversal symmetry) as a function of two parameters, pairs of levels typically become degenerate at isolated points in the parameter space [1]. These points have been termed "diabolical points" [2] because of the double-cone structure of the intersecting energy-level surfaces, which was first described by Teller [3]. These degeneracies and near-degeneracies are physically significant because they can facilitate nonadiabatic (Landau-Zener) transitions in systems where the parameters are a slowly varying function of time [4]. These effects are important in "radiationless transitions" between potential surfaces of molecules [5], and it has also been proposed that they can act as a mechanism for dissipation in nuclear collisions [6].

The spectra of systems which have a large number of levels typically have the same short-ranged statistical properties as the eigenvalues of certain random-matrix ensembles. Significant exceptions, which we will not consider further, occur when there are symmetries, quantization conditions due to tori in the classical phase space [7], or when states are Anderson localized [8]. We consider a system with time-reversal invariance and in which the Hamiltonian does not depend on spin, for which the spectral statistics typically resemble those of the Gaussian orthogonal ensemble (GOE). The properties of the GOE and other random-matrix models are described in detail in a reprint volume by Porter [9]. Motivated largely by the desire to understand the response of complicated quantum systems to time-dependent changes of their parameters [10,11], this statistical approach has been extended to consider the parameter dependence of energy levels. The density in the parameter space of avoided crossings can be calculated analytically for a parameter-dependent GOE model, and for semiclassical systems the parameters of the model can be related to a classical correlation function [12]. Some other statistical aspects of the parameter dependence of energy levels have been considered by Gaspard *et al.* [13], using an equation-of-motion description of a parameter-dependent GOE devised by Pechukas [14]. The parametrized GOE model has been shown to give a very good description of both the statistics of the matrix elements and the parameter dependence of the energy levels in a chaotic quantum billiard system [15]. In this paper we extend the analysis of the parametrized GOE model to two-parameter systems. We calculate the density of diabolical points in parameter space, and also the joint distribution of the slopes and eccentricities of the associated conical intersections of pairs of energy levels. The results greatly extend a very simple estimate for the density of diabolical points obtained previously [2].

As well as giving useful information about two-parameter systems, this calculation also helps to clarify a point connected with the density of avoided crossings. Recently some numerical results have been reported which are at variance with a prediction of the parametrized GOE model. This model predicts that the density of avoided crossings with minimal separations of successive levels less than Δ is proportional to Δ in the limit $\Delta \to 0$; it has been claimed [16,17] that this distribution vanishes faster than linearly as $\Delta \to 0$. In Sec. II of this paper we discuss the relationship between the avoided crossings and nearby diabolical points, and show that the scaling of the density of avoided crossings in this limit can be derived from the same very minimal assumptions as used by Wigner [18] (also reprinted in the volume by Porter [9]) to derive the linear repulsion of energy levels.

In Sec. III we obtain a general expression for the density of diabolical points, and obtain an explicit result for the parametrized GOE model. Appendixes A and B contain a discussion of how this result can be applied to

 ©1993 The American Physical Society

obtain the semiclassical density of diabolical points for a two-parameter classically chaotic quantum system. In Sec. IV we obtain the joint probability distribution for the eccentricities and slopes of the conical intersections associated with the diabolical points for the parametrized GOE system. The analysis is similar in approach to that used by Rice [19] and Longuet-Higgins [20] to investigate the topography of Gaussian random functions. Numerical results reported in Sec. V confirm the correctness of these expressions. In Sec. V we also report some numerical investigations of the distribution of spacings between diabolical points in parameter space: surprisingly, diabolical points on the same energy surface do not exhibit repulsion at small separations. A scaling argument is presented which explains this result.

Some results on a related problem have been obtained recently for systems without time-reversal symmetry, where energy levels become degenerate if three parameters are varied. These degeneracies have a sign associated with them, which is related to the two-form describing the evolution of the phase of the wave function under adiabatic changes of the parameters [21,22]. The signed density of these three-parameter degeneracies can be evaluated using a trace identity [23].

II. DEGENERACIES AND NEAR-DEGENERACIES IN A TWO-PARAMETER SYSTEM

We consider a system with a Hamiltonian depending on two parameters, $\hat{H}(X_1, X_2)$, which has time-reversal symmetry, and which has no symmetries or constants of motion. The eigenvalues $E_n(X_1, X_2)$ become degenerate at isolated points in the (X_1, X_2) plane. Consider the behavior of the energy levels in the neighborhood of one of these degeneracies, where the pair of eigenvalues E_n, E_{n+1} become degenerate at a nearby point $\mathbf{X}^* = (X_1^*, X_2^*)$. According to degenerate perturbation theory, the energy levels in the neighborhood of $\mathbf{X}^*$ are given by the eigenvalues of a 2×2 matrix

$$\begin{pmatrix} E_n^* + V_{n,n} & V_{n,n+1} \\ V_{n,n+1} & E_n^* + V_{n+1,n+1} \end{pmatrix}, \tag{2.1}$$

where $E_n^* = E_n(\mathbf{X}^*)$, and the $V_{n,n'}$ are matrix elements of $\hat{V} = (\partial \hat{H}/\partial \mathbf{X}) \cdot \delta \mathbf{X}$, in the basis formed by the eigenstates of $\hat{H}(\mathbf{X}^*)$, with $\delta \mathbf{X} = \mathbf{X} - \mathbf{X}^*$. The separation Δ of the two eigenvalues of this matrix is

$$\begin{aligned} \Delta &= \sqrt{(V_{n,n} - V_{n+1,n+1})^2 + 4V_{n,n+1}^2} \\ &= \sqrt{[(d\hat{H}/d\mathbf{X})_d \cdot \delta \mathbf{X}]^2 + 4[(d\hat{H}/d\mathbf{X})_o \cdot \delta \mathbf{X}]^2}, \end{aligned} \tag{2.2}$$

where

$$\begin{aligned} (d\hat{H}/d\mathbf{X})_d &= (d\hat{H}/d\mathbf{X})_{n,n} - (d\hat{H}/d\mathbf{X})_{n+1,n+1}, \\ (d\hat{H}/d\mathbf{X})_o &= (d\hat{H}/d\mathbf{X})_{n,n+1} \ . \end{aligned} \tag{2.3}$$

Note that Δ^2 is a quadratic form in $(\delta X_1, \delta X_2)$; the region of the (X_1, X_2) plane in the neighborhood of this degeneracy for which the separation of the two levels is less than Δ is therefore an ellipse of area

$$A = \frac{\pi}{2}\Delta^2 \Big/ \left[\left(\frac{\partial \hat{H}}{\partial X_1}\right)_d \left(\frac{\partial \hat{H}}{\partial X_2}\right)_o - \left(\frac{\partial \hat{H}}{\partial X_2}\right)_d \left(\frac{\partial \hat{H}}{\partial X_1}\right)_o \right]. \tag{2.4}$$

In the following paragraphs, it will be assumed that there are a large number of degeneracies, with a density $\mathcal{D}$ in the parameter space: more precisely the number of degeneracies connecting one energy surface $E_n(\mathbf{X})$ with the energy-level surface $E_{n+1}(\mathbf{X})$ above it is $\mathcal{D}$ per unit area of the parameter space. The consequences for the distribution of close level spacings and the density of avoided crossings will now be considered.

Consider first how the level-spacing distribution is related to this assumption. The level-spacing distribution can be evaluated in various ways, for example by averaging over the energy levels, by averaging over a line in the parameter space, or by averaging over the entire parameter space. An "ergodic" assumption will be made, namely that the same level-spacing distribution will be produced by any of these averaging procedures. An ergodic property similar to that being invoked here has been proved for the GOE random-matrix model [24]. The level-spacing distribution at small spacings can be computed most easily by averaging over the two-parameter space. The proportion of the energy levels with separations below Δ is given by the fraction of the area of the (X_1, X_2) plane for which the separation is less than Δ. In the limit $\Delta \to 0$ this is equal to the density of diabolical points multiplied by the mean value of the elliptical area A attached to each one satisfying $E_{n+1} - E_n < \Delta$. Figure 1 is a schematic illustration of these elliptical regions surrounding diabolical points (the positions and orientations are derived from the model described in Sec. V, but for visibility all of the ellipses are drawn with the same area). From (2.4), the area of each ellipse, and therefore the mean area, is proportional to the square of Δ. The

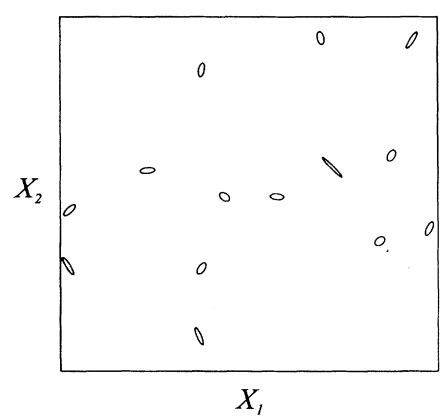

FIG. 1. Schematic illustration of the regions of the parameter space where the separation of two successive energy levels is less than Δ: this is a set of elliptically shaped regions when Δ is much smaller than the mean level spacing.

level-spacing distribution, which is the derivative of this cumulative distribution, is therefore proportional to Δ for small spacings. This was one of the arguments originally used by Wigner [18] to justify his surmise about the level-spacing distribution. In Sec. III of this paper we turn Wigner's argument around, and use the current more refined knowledge about the level-spacing distribution to deduce the density of diabolical points.

Consider next the calculation of the density of avoided crossings. This is the number of times per unit length that the separation $E_{n+1} - E_n$ of a given pair of levels falls below Δ as we traverse a given line in parameter space. We can again use an ergodic assumption, namely that this statistic will be the same for any line drawn in a given direction in (X_1, X_2) space. This assumption will be valid if the distribution of the diabolical points in the parameter space resembles a random distribution of points; this is certainly correct for the GOE model, and presumably also valid for systems with GOE-like energy-level statistics. Using this ergodic assumption, the density of avoided crossings is equal to the density of diabolical points multiplied by the "cross section" for the line to bisect a given ellipse. The cross section is clearly the mean value of the projection of the ellipses in a direction perpendicular to the line of section: this quantity is proportional to Δ, because the linear dimension of each ellipse is proportional to Δ. The scaling of the density of avoided crossings (although not the numerical prefactor) can therefore be obtained by simple geometrical considerations, starting from a very minimal assumption of ergodicity.

Recently two papers [16,17] have appeared containing numerical results which are at variance with this prediction, claiming that a statistic closely related to the density of avoided crossings does not scale in the manner predicted above. As well as being at variance with the theory, these results also disagree with our own numerical results which verify both the scaling and the prefactor [15]. Neither of these papers offers a satisfactory explanation of the surprising numerical results presented.

III. CALCULATION OF THE DENSITY OF DIABOLICAL POINTS

In this section we derive the density of diabolical points for a two-parameter Hamiltonian $\hat{H}(X_1, X_2)$ with time-reversal symmetry. A scaling law for the density of diabolical points as a function of the level number has previously been obtained for the specific case of a quantum billiard [2]. Because we have to consider many different probability distributions, we will adopt the convention in the remainder of this paper that $P[\ ]$ denotes the probability distribution of the variable(s) enclosed in square brackets.

The following calculations involve both the eigenvalues of the operator $\hat{H}(\mathbf{X})$, and the matrix elements of $\partial\hat{H}/\partial X_i$ in the basis formed by the eigenstates of $\hat{H}(\mathbf{X})$. Both of these quantities are regarded as random variables. The results given below are based on the assumption that the matrix elements are independent of the eigenvalues. This assumption can easily be verified for the parametrized GOE model discussed in Sec. V. It is also satisfied in the Pechukas description of a parameter dependent GOE [14].

We now consider how to compute the density of degeneracies. Assume that two levels labeled 1 and 2 with energies E_1, E_2, $|E_2 - E_1| = \Delta$, situated at $X_1 = X_2 = 0$, are sufficiently close to a degeneracy that degenerate perturbation theory (2.1)–(2.3) can be applied. The distance R in the parameter space from the origin to the degeneracy can be obtained as

$$R = \frac{2\Delta}{|d|}\left[\left(\frac{\partial H}{\partial X_1}\right)_o^2 + \left(\frac{\partial H}{\partial X_2}\right)_o^2\right]^{1/2} = f\Delta, \tag{3.1}$$

where the notation of (2.3) has been used and

$$d = 2\left[\left(\frac{\partial H}{\partial X_1}\right)_d\left(\frac{\partial H}{\partial X_2}\right)_o - \left(\frac{\partial H}{\partial X_2}\right)_d\left(\frac{\partial H}{\partial X_1}\right)_o\right]. \tag{3.2}$$

Expression (3.1) shows that the distance from a near-degeneracy of size Δ to a degeneracy is proportional to Δ. To determine the density of degeneracies it is necessary to average over f, which is a function of the matrix element combinations defined in (2.3), and over the level-spacing distribution $P[\Delta]$ to find the probability of a given R. Because f is a function of the matrix elements only, f and Δ are independently distributed, so that

$$P[R] = \int_0^\infty df \int_0^\infty d\Delta\ P[f]\ P[\Delta]\ \delta(R - f\Delta). \tag{3.3}$$

Using the scaling of the level-spacing distribution discussed in Sec. II,

$$P[\Delta] = \gamma\ \Delta \tag{3.4}$$

(3.3) can be expressed as

$$\begin{aligned} P[R] &= \int_0^\infty df\ P[f]\ f^{-1} \int_0^\infty d\Delta\ P[\Delta]\ \delta\left(\Delta - \frac{R}{f}\right) \\ &= \int_0^\infty df\ P[f]\ f^{-1} \int_0^\infty d\Delta\ \gamma\ \Delta\ \delta\left(\Delta - \frac{R}{f}\right) \\ &= \int_0^\infty df\ P[f]\ f^{-2}\ \gamma R \\ &= \gamma R \langle f^{-2}\rangle. \end{aligned} \tag{3.5}$$

Because (3.4) is only valid for Δ small compared to the typical level spacing, (3.5) is only valid for small R. [The Dirac δ functions in (3.5) imply that the support of the integrand does not extend to large values of Δ where the approximation (3.4) breaks down.] The density of degeneracies can now be obtained in terms of $P[R]$. Let $\mathcal{D}$ be the density of degeneracies and $\mathcal{N}$ the number of degeneracies found in a circle of radius R in the parameter space. This has expectation value

$$\langle\mathcal{N}\rangle = \pi R^2 \mathcal{D}. \tag{3.6}$$

The probability of finding a degeneracy between R and $R + dR$ is $d\langle\mathcal{N}\rangle/dR$ so

$$P[R]\ dR = 2\pi\mathcal{D}\ dR = \gamma\langle f^{-2}\rangle R\ dR. \tag{3.7}$$

This implies that

$$\mathcal{D} = \frac{\gamma\langle f^{-2}\rangle}{2\pi}. \tag{3.8}$$

To obtain the final form of $P[R]$ and hence of $\mathcal{D}$, it is necessary to find the average value of f^{-2}. In terms of the matrix elements this quantity is

$$\langle f^{-2}\rangle = \left\langle \frac{A^2D^2 + B^2C^2 - 2ABCD}{C^2 + D^2} \right\rangle, \tag{3.9}$$

where

$$A = \left(\frac{\partial H}{\partial X_1}\right)_d, \quad B = \left(\frac{\partial H}{\partial X_2}\right)_d,$$
$$C = 2\left(\frac{\partial H}{\partial X_1}\right)_o, \quad D = 2\left(\frac{\partial H}{\partial X_2}\right)_o. \tag{3.10}$$

In order to proceed further it is necessary to consider the statistical properties of A, B, C, and D. We assume that the matrix elements of $(\partial\hat{H}/\partial X_1)$ and $(\partial\hat{H}/\partial X_2)$ are uncorrelated. (The more general case of correlated X_1 and X_2 derivatives is discussed later.) With this assumption the cross term $ABCD$ in (3.9) will average to zero and the average values of the products of uncorrelated quantities can be factored,

$$\begin{aligned}\langle f^{-2}\rangle &= \left\langle \frac{A^2D^2 + B^2C^2}{C^2 + D^2} \right\rangle \\ &= \langle A^2\rangle\left\langle \frac{D^2}{C^2 + D^2} \right\rangle + \langle B^2\rangle\left\langle \frac{C^2}{C^2 + D^2} \right\rangle.\end{aligned} \tag{3.11}$$

To obtain a specific prediction of the density of degeneracies the above results are now specialized to the case where the matrix elements of $(\partial\hat{H}/\partial X_1)$ and $(\partial\hat{H}/\partial X_2)$ conform to a GOE model, i.e., the off-diagonal and diagonal elements of these matrices are Gaussian distributed with variances σ^2 and $2\sigma^2$, respectively. For this model, A, B, C, and D are all independently Gaussian distributed with variance $4\sigma^2$. These properties allow (3.11) to be written as

$$\langle f^{-2}\rangle = 2\langle A^2\rangle\left\langle \frac{D^2}{D^2 + C^2} \right\rangle = 8\sigma^2\left\langle \frac{D^2}{D^2 + C^2} \right\rangle. \tag{3.12}$$

The average over C and D is

$$\frac{1}{2\pi\sigma^2}\int_{-\infty}^{\infty} dC \int_{-\infty}^{\infty} dD \frac{D^2}{D^2 + C^2} \exp[-(C^2+D^2)/2\sigma^2] = \tfrac{1}{2} \tag{3.13}$$

and therefore

$$P[R] = 4\sigma^2\gamma R. \tag{3.14}$$

Using the explicit form of the level-spacing distribution coefficient for the GOE [9], $\gamma = \pi^2 n_0^2/6$, the density of degeneracies is therefore

$$\mathcal{D} = \tfrac{1}{3}\pi n_0^2\sigma^2, \tag{3.15}$$

where n_0 is the smoothed density of states.

For a general Hamiltonian, the matrix elements of $(\partial\hat{H}/\partial X_1)$ and $(\partial\hat{H}/\partial X_2)$ will have different variances σ_{11}^2 and σ_{22}^2, and they will also have a nonzero correlation σ_{12}^2. This more general case can be dealt with by making a suitable transformation of the coordinate space, such that in the new coordinates $\sigma_{1'1'}^2 = \sigma_{2'2'}^2 = 1$ and $\sigma_{1'2'}^2 = 0$. This is described in Appendix A: the results show that the general expression for $\mathcal{D}$ is

$$\mathcal{D} = \tfrac{1}{3}\pi n_0^2(\sigma_{11}\sigma_{22} - \sigma_{12}^2). \tag{3.16}$$

If the system under consideration is a semiclassical system with a chaotic classical limit, the variances σ^2 can be obtained from certain classical correlation functions. This is described in Appendix B.

IV. DISTRIBUTION OF CONE PARAMETERS

The method described in Sec. III can be extended to give the joint distribution of the parameters describing the variation of the separation of the two energies in the neighborhood of the degeneracy.

In terms of the notation of Sec. III, the separation Δ of the two energy levels is given by

$$\begin{aligned}\Delta^2 = &(A^2 + C^2)\delta X_1^2 + (B^2 + D^2)\delta X_2^2 \\ &+2(AB + CD)\delta X_1\delta X_2,\end{aligned} \tag{4.1}$$

where A, B, C, D are defined by (3.10): note that Δ^2 is a quadratic form in $(\delta X_1, \delta X_2)$, so that the level lines of Δ are ellipses. We now consider the distribution of the parameters of the quadratic form (4.1) for the parametrized GOE model. We will assume, as in Sec. III, that the coordinate system (X_1, X_2) has been chosen (using the method described in Appendix A) so that the statistics of the model are isotropic. The cones are most conveniently described in terms of the eccentricity of the elliptical level lines of Δ, the angle of the major axis of this ellipse to a reference direction, and a parameter s describing the slope of the cone. Because the model is isotropic, the distribution of angles is obviously uniform. The two other parameters can be obtained from the eigenvalues of the matrix characterizing the quadratic form (4.1),

$$\tilde{A} = \begin{pmatrix} A^2 + C^2 & AB + CD \\ AB + CD & B^2 + D^2 \end{pmatrix}. \tag{4.2}$$

We characterize the eccentricity of the ellipse by the ratio ϵ of the lengths of the minor and major axes; this quantity is related to the eigenvalues λ_+, λ_- by $\epsilon = \sqrt{\lambda_-/\lambda_+}$ (with $\lambda_- \le \lambda_+$ so that $\epsilon \le 1$). The slope of the cone is conveniently characterized by the inverse of the ratio of the area of the ellipse to Δ, which is proportional to $d^2 = \lambda_+\lambda_-$. It is not very convenient to compute the joint probability distribution of ϵ and s directly; instead we compute the distribution of the parameters

$$\begin{aligned} t &= \mathrm{tr}(\tilde{A}) = A^2 + B^2 + C^2 + D^2, \\ d &= \sqrt{\det(\tilde{A})} = AD - BC. \end{aligned} \tag{4.3}$$

These can be related to ϵ and s using the following relation for the eigenvalues in terms of t and d:

$$\lambda_\pm = \tfrac{1}{2}(t \pm \sqrt{t^2 - d^2}). \tag{4.4}$$

By a simple extension of the argument leading to (3.8), the density of diabolical points with t between t_0 and $t_0 + \delta t_0$, and with d between d_0 and $d_0 + \delta d_0$, is

$$\mathcal{D}(t_0, d_0)\ \delta t_0\ \delta d_0 = \frac{\gamma}{2\pi}\delta t_0\ \delta d_0 \int_{-\infty}^{\infty} dA \int_{-\infty}^{\infty} dB \int_{-\infty}^{\infty} dC \int_{-\infty}^{\infty} dD\ P[A,B,C,D]\frac{(AD-BC)^2}{C^2+D^2}\ \delta(t_0 - t)\ \delta(d_0 - d), \tag{4.5}$$

where $P[A,B,C,D]$ is the joint distribution of A, B, C, D. For the GOE model these variables are independently distributed with mean zero and variance $4\sigma^2$. The joint probability density $P[t,d]$ is obtained by dividing $\mathcal{D}(t,d)$ by the total density $\mathcal{D}$ given by (3.15). The integral in (4.5) is most conveniently evaluated by integrating over C and D first, then over A and B: write

$$\begin{aligned} P[t_0, d_0] &= \frac{1}{256\pi^2\sigma^6} I(t_0, d_0), \\ I(t_0, d_0) &= \int_{-\infty}^{\infty} dA \int_{-\infty}^{\infty} dB\ e^{-(A^2+B^2)/8\sigma^2}\ J(\tau_0, d_0, A, B), \\ J(\tau_0, d_0, A, B) &= \int_{-\infty}^{\infty} dC \int_{-\infty}^{\infty} dD\ e^{-(C^2+D^2)/8\sigma^2} \frac{d^2}{C^2+D^2}\ \delta(d_0 - d)\ \delta(\tau_0 - C^2 - D^2), \end{aligned} \tag{4.6}$$

where $\tau = t - (A^2 + B^2)$. We calculate the integral J by performing a rotation in the C, D plane, such that in the transformed coordinates, C', D',

$$d(A, B, C', D') = \sqrt{A^2 + B^2}\ C'. \tag{4.7}$$

The integral J can now be computed by transforming the C', D' plane to polar coordinates, (r, θ),

$$\begin{aligned} J(\tau, d, A, B) &= \int_{-\infty}^{\infty} dC' \int_{-\infty}^{\infty} dD'\ e^{-(C'^2+D'^2)/8\sigma^2} \frac{(A^2+B^2)C'^2}{C'^2+D'^2} \delta(d - \sqrt{A^2+B^2}\ C')\ \delta(\tau - C'^2 - D'^2) \\ &= \tfrac{1}{2} e^{-\tau/8\sigma^2} \int_0^{2\pi} d\theta \cos^2\theta\ \delta(\sqrt{\tau(A^2+B^2)}\cos\theta + d) = e^{-\tau/8\sigma^2} \frac{d^2}{\tau\sqrt{\tau(A^2+B^2) - d^2}}. \end{aligned} \tag{4.8}$$

The integral $I(t,d)$ can now be evaluated easily in polar coordinates

$$I(t,d) = \int_0^{2\pi} d\theta \int_{r_1}^{r_2} dr\ r e^{-t/8\sigma^2} \frac{d^2}{t - r^2} \frac{1}{\sqrt{(t-r^2)r^2 - d^2}} = \pi e^{-t/8\sigma^2} t\alpha^2 F(\alpha), \tag{4.9}$$

where $\alpha = d/t$ and the range of the inner integral of (4.9) is such that the square root remains real, and

$$F(\alpha) = \int_{x_-}^{x_+} dx\ \frac{1}{x} \frac{1}{\sqrt{[x(1-x) - \alpha^2]}}, \tag{4.10}$$

with $x_\pm = \frac{1}{2}(1 \pm \mu)$, $\mu = \sqrt{(1 - 4\alpha^2)}$. The successive substitutions $X = (2x-1)/\mu$, $X = \sin\theta$, allow $F(\alpha)$ to be obtained as a standard integral

$$\begin{aligned} F(\alpha) = 2\int_{-1}^{1} dX \frac{1}{(\mu X + 1)\sqrt{1 - X^2}} &= 2\int_{-\pi/2}^{\pi/2} d\theta \frac{1}{1 + \mu\sin\theta} \\ &= \frac{4}{\sqrt{1-\mu^2}} \left[\arctan\left(\frac{1+\mu}{\sqrt{1-\mu^2}}\right) + \arctan\left(\frac{1-\mu}{\sqrt{1-\mu^2}}\right)\right]. \end{aligned} \tag{4.11}$$

Substituting for μ in terms of α gives the simple result

$$F(\alpha) = \frac{\pi}{\alpha}\ . \tag{4.12}$$

Finally, substituting into (4.9) and (4.6) we have

$$P[t,d] = \frac{d}{256\sigma^6} e^{-t/8\sigma^2}. \tag{4.13}$$

We now use this result to obtain the distribution of the axis ratio ϵ of the ellipses. The probability distribution

$P[\alpha]$ can be obtained as

$$\begin{aligned} P[\alpha] &= \int_0^\infty dt \int_{-\infty}^\infty dd\ \delta\left(\alpha - \frac{d}{t}\right)\ P[t,d] \\ &= \int_0^\infty dt t P[t, \alpha t] \\ &= \frac{\alpha}{256\sigma^2}\int_0^\infty dt\ t^2 e^{-t/8\sigma^2} = 4\alpha. \end{aligned} \tag{4.14}$$

The relationship between α and ϵ defined previously can now be used to obtain the probability distribution for ϵ,

$$P[\epsilon] = \frac{2\sin\left[4\arctan(\epsilon)\right]}{1+\epsilon^2} = \frac{8\epsilon(1-\epsilon^2)}{(1+\epsilon^2)^3}. \tag{4.15}$$

The eccentricity e is related to ϵ by $e = \sqrt{1-\epsilon^2}$. The probability distribution for e can be obtained from (4.15) as

$$P[e] = \left(\frac{2e}{2-e^2}\right)^3. \tag{4.16}$$

V. NUMERICAL INVESTIGATIONS

We investigated the density and other properties of diabolical points numerically by considering the two-parameter Hamiltonian

$$\begin{aligned} \hat{H} = &\ \hat{H}_1\cos(X_1) + \hat{H}_2\sin(X_1) + \hat{H}_3\cos(X_2) \\ &+ \hat{H}_4\sin(X_2) \end{aligned} \tag{5.1}$$

with $\hat{H}_1$, $\hat{H}_2$, $\hat{H}_3$ and $\hat{H}_4$ different realizations of the GOE, with matrix dimension M and with an off-diagonal variance of unity. The Hamiltonian $\hat{H}$ and its derivatives $(\partial\hat{H}/\partial X_1)$, $(\partial\hat{H}/\partial X_2)$ are independent GOE matrices. This Hamiltonian conforms to GOE statistics with the variance of the off-diagonal matrix elements equal to 2, and the variances associated with the matrix elements of the derivatives of $\hat{H}$ with respect to X_1 and X_2 are $\sigma_{11}^2 = \sigma_{22}^2 = 1$, $\sigma_{12}^2 = 0$. The number and positions of the degeneracies of the eigenvalues of $\hat{H}$ were found by performing a search in the (X_1, X_2) plane. Figure 1 shows some typical results: we have plotted an ellipse corresponding to a level line of Δ around the position of each diabolical point (for clarity, the sizes of the ellipses have been magnified, and they are all drawn with the same area). The data for this figure are the diabolical points between levels 1 and 2 of a realization of (5.1) with matrix dimension $M = 20$.

By calculating the number of diabolical points as a function of the matrix dimension, it is possible to test the result (3.15) derived above. Expression (3.15) gives the density of degeneracies for a pair of levels in terms of the local density of states n_0. To convert this to the total number of degeneracies, it is necessary to obtain a sum over all levels and the whole parameter space. The variances are independent of energy in this model but the density of states is energy dependent. The parameter space has area $4\pi^2$, so the total number of degeneracies $\mathcal{N}$ is

$$\begin{aligned} \mathcal{N} &= \sum_{n=1}^{M-1}\mathcal{N}_n = \frac{4\pi^3\sigma^2}{3}\sum_{n=1}^{M-1} n_0^2(E_n) \\ &= \frac{4\pi^3\sigma^2}{3}\int_1^{M-1} dn\ n_0^2(E_n) \\ &= \frac{4\pi^3\sigma^2}{3}\int_{-\infty}^{\infty} dE\ \frac{dn}{dE} n_0^2 \\ &= \frac{4\pi^3\sigma^2}{3}\int_{-\infty}^{\infty} dE\ n_0^3(E). \end{aligned} \tag{5.2}$$

For the Hamiltonian (5.1) n_0 is given by

$$n_0(E) = \frac{\sqrt{M}}{\sqrt{2}\pi}\left(1 - \frac{E^2}{8M}\right)^{1/2} \tag{5.3}$$

in the limit $M \to \infty$ [9], so that the required integral is

$$\left(\frac{M}{2}\right)^{3/2}\frac{1}{\pi^3}\int_{-2\sqrt{2}M}^{2\sqrt{2}M} dE\ \left(1 - \frac{E^2}{8M}\right)^{3/2} = \frac{3M^2}{8\pi^2}. \tag{5.4}$$

Substituting into (5.2) and putting $\sigma = 1$ gives the number of degeneracies as

$$\mathcal{N} = \frac{\pi}{2}M^2. \tag{5.5}$$

Table I shows a comparison of the calculated number of degeneracies and the number predicted from (5.5) for a range of matrix sizes M; the agreement can be seen to be excellent.

The equation of the quadratic form (4.1) can readily be found by making small variations of X_1 and X_2 in the vicinity of each diabolical point; the axis ratio of the ellipse can then be obtained from the eigenvalues of the corresponding matrix (4.2). The results are shown in Fig. 2: they are in excellent agreement with the theoretical prediction, (4.15). The data were obtained for diabolical points from four realizations of the Hamiltonian (5.1) with matrix dimension 50.

We also investigated the distribution of spacings in the parameter space between neighboring diabolical points, by computing the cumulative distribution of distances r from a given diabolical point between levels $n, n+1$, to its nearest neighbor between levels $n+N, n+N+1$. For randomly distributed points this cumulative distribution is

TABLE I. Number of diabolical points for the Hamiltonian (5.1) averaged over five GOE realizations for a range of matrix dimensions, compared with the prediction (5.5). The ratio $\mathcal{N}_{\rm obs}/\mathcal{N}_{\rm calc}$ approaches unity as the matrix dimension increases.

N	$\mathcal{N}_{\rm obs}$	$\mathcal{N}_{\rm calc}$	$\mathcal{N}_{\rm obs}/\mathcal{N}_{\rm calc}$
5	35	39	0.90
10	144	157	0.92
20	564	598	0.94
30	1370	1414	0.97
40	2489	2513	0.99
50	3847	3927	0.98

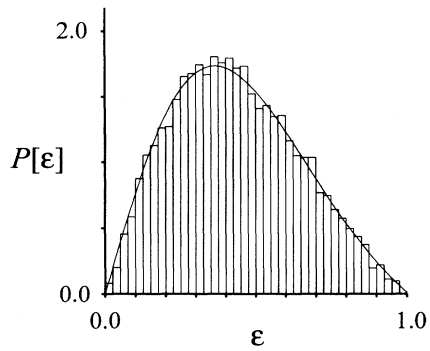

FIG. 2. Distribution of axis ratios of diabolical points for the GOE model (histogram), compared with the theoretical distribution (4.15) (smooth curve).

$$Q[r] = 1 - e^{-\pi \mathcal{D} r^2}, \tag{5.6}$$

which is quadratic for small values of the distance r. The results are shown in Fig. 3, for points on the same level, $N = 0$, and the first and second nearest neighbors, $N = 1, 2$, with (5.6) for comparison. The data set used was as for Fig. 2. The distances were scaled so that the mean density of diabolical points is unity. Surprisingly, there is no repulsion between diabolical points on the same energy-level surface. Diabolical points between neighboring levels show a clear repulsion, and from the second neighbor onwards the results show increasingly good agreement with (5.6).

We now present a simple scaling argument for the fact that diabolical points on the same level surface do not exhibit repulsion. Although it is possible to refine this argument considerably, we have not succeeded in finding an exact relation for the cumulative spacing distribution, $Q[r]$, even for small r. In the neighborhood of a diabolical point degenerate perturbation theory can be applied to the separation Δ between two levels. The separation is given by the eigenvalues $\pm\frac{1}{2}\Delta$ of a 2×2 matrix,

$$\tilde{M} = \begin{pmatrix} F(X_1, X_2) & G(X_1, X_2) \\ G(X_1, X_2) & -F(X_1, X_2) \end{pmatrix}, \qquad \Delta = \sqrt{F^2 + G^2}. \tag{5.7}$$

The separation Δ vanishes when both F and G vanish, at isolated points in the (X_1, X_2) plane. Two diabolical points will lie close together if the zero level lines of $F(X_1, X_2)$ and $G(X_1, X_2)$ are nearly parallel, and if the lines have some degree of curvature which causes them to cross again: this is illustrated in Fig. 4. If the coordinates in parameter space are scaled so that the mean density $\mathcal{D}$ is unity, the typical radii of curvature of these lines is also of order unity. The two diabolical points will be close together if the angle between the level curves of F and G is small: if this angle is θ the distance r between the diabolical points is of order θ (see Fig. 4). The angle θ is proportional to the axis ratios ϵ of the pair of nearby diabolical points if ϵ is small. We therefore have $r \sim \theta \sim \epsilon$ for pairs of nearby diabolical points. From (4.15), the probability distribution of ϵ is linear for small ϵ. The probability distribution of r is therefore also linear for small r, and its cumulative distribution is quadratic,

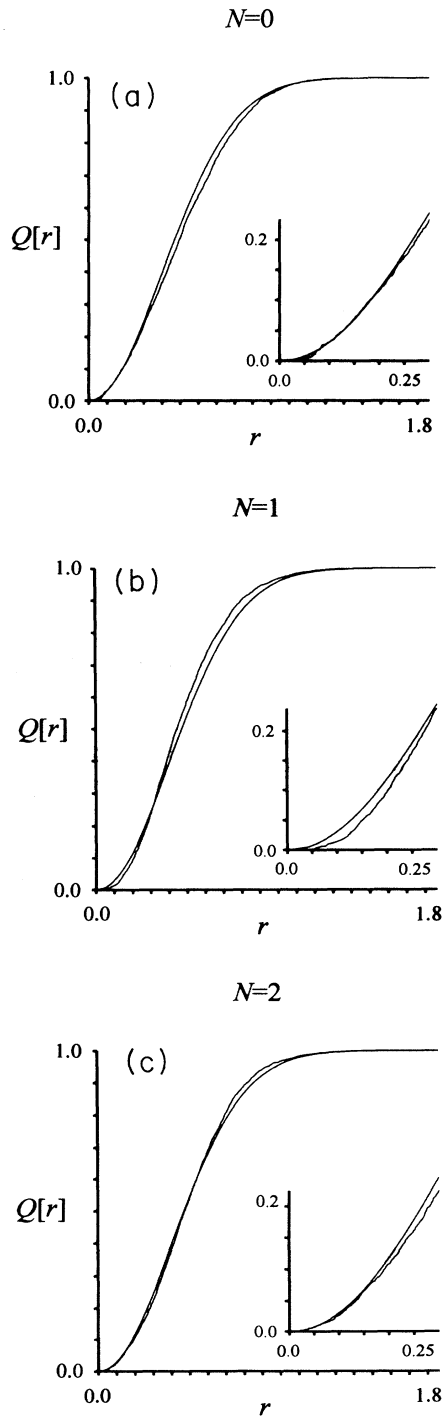

FIG. 3. Cumulative distribution of the distance r from a given diabolical point on the nth level to its nearest neighbor on the $(n + N)$th level, for the three cases (a) $N = 0$, (b) $N = 1$ (c), $N = 2$. The smooth curves are the distribution for a random scatter of points.

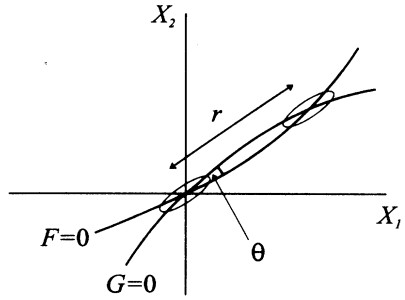

FIG. 4. Schematic illustration of the geometry of two closely spaced diabolical points, discussed in Sec. V. The elliptical level curves of Δ are aligned for nearby pairs of diabolical points.

in agreement with (5.6). The numerical results shown in Fig. 3(a) are consistent with the hypothesis that the coefficient of this quadratic dependence is the same as for the random distribution, (5.6).

This simple argument also predicts that both the eccentricities and the orientations of the ellipses associated with closely spaced diabolical points are correlated. This was confirmed by plotting these elliptical regions in the same manner as for Fig. 1, for a case where the density of diabolical points is larger; the results are shown in Fig. 5. A number of examples of this correlation can be seen: ellipses with small ϵ usually occur as pairs with both of their longer axes aligned with the line joining their centers, as illustrated in Fig. 4. (Some of the ellipses overlap in this figure because the diabolical points are very close together.) The data for this figure used the diabolical points connecting levels 9 and 10 of a realization of (5.1) with dimension $M = 20$.

We can also give a simple scaling argument for the small-r behavior for diabolical points on nearest-neighboring levels. Consider a pair of levels (1 and 2, say), which become very nearly degenerate at $X_1 = X_2 = 0$, with a separation less than δE. Assume that there is a third level with a separation in energy Δ from levels 1 and 2, which is large compared to δE but small compared to the mean level spacing. Levels 2 and 3 will meet at a diabolical point a distance $r \sim \Delta$ away in the parameter space. The probability distribution of r is therefore proportional to the probability distribution of Δ. Dyson's result [25] for the joint probability density of energy levels of the GOE contains a term in the product of differences of energy levels: for three levels

$$P[E_1, E_2, E_3] \approx (E_1 - E_2)(E_1 - E_3)(E_2 - E_3). \tag{5.8}$$

The probability density for the third level to be at a distance Δ from the very near degeneracy at $X_1 = X_2 = 0$ is therefore proportional to Δ^2. The probability density of the spacings r is therefore proportional to r^2 for small r, leading to a cumulative distribution proportional to r^3. The results shown in Fig. 3(b) are consistent with this conclusion in that they show a "repulsion" of nearby degeneracies, but we could not obtain enough data to verify the small-r behavior unambiguously.

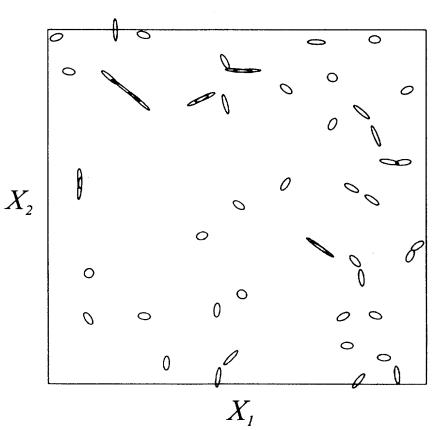

FIG. 5. Similar to Fig. 1, showing the correlation of the alignments and eccentricities of nearby diabolical points.

ACKNOWLEDGMENTS

Research grants by the U.K. Science and Engineering Research Council and the University of Strathclyde are gratefully acknowledged.

APPENDIX A

Assume that in coordinates (X_1', X_2') the matrix elements of $(\partial\hat{H}/\partial X_1')$, $(\partial\hat{H}/\partial X_2')$ satisfy

$$\begin{aligned}
&\left\langle \left(\frac{\partial\hat{H}}{\partial X_1'}\right)^2_{nm} \right\rangle = \sigma^2_{1'1'} = 1, \\
&\left\langle \left(\frac{\partial\hat{H}}{\partial X_2'}\right)^2_{nm} \right\rangle = \sigma^2_{2'2'} = 1, \\
&\left\langle \left(\frac{\partial\hat{H}}{\partial X_1'}\right)_{nm} \left(\frac{\partial\hat{H}}{\partial X_2'}\right)_{nm} \right\rangle = \sigma^2_{1'2'} = 0.
\end{aligned} \tag{A1}$$

We consider the transformation to a set of coordinates (X_1, X_2) defined by the linear transformation

$$\begin{pmatrix} X_1' \\ X_2' \end{pmatrix} = \begin{pmatrix} \alpha & \beta \\ \gamma & \delta \end{pmatrix} \begin{pmatrix} X_1 \\ X_2 \end{pmatrix}. \tag{A2}$$

The matrix elements of the derivative of $\hat{H}$ with respect to X_1 satisfy

$$\begin{aligned}
\left\langle \left(\frac{\partial\hat{H}}{\partial X_1}\right)^2_{nm} \right\rangle &= \sigma^2_{11} \\
&= \alpha^2\sigma^2_{1'1'} + 2\alpha\beta\sigma^2_{1'2'} + \beta^2\sigma_{2'2'} \\
&= \alpha^2 + \beta^2
\end{aligned} \tag{A3}$$

and similarly

$$\sigma^2_{22} = \gamma^2 + \delta^2, \quad \sigma^2_{12} = \alpha\gamma + \beta\delta. \tag{A4}$$

For a given physical system the variances σ^2_{11}, σ^2_{12}, σ^2_{22} of the matrix elements are given, and the parameters α, β, γ, δ defining the transformation to the (X_1', X_2') coordinates are unknown. The fact that there are four param-

eters and only three unknowns is unimportant, because the fourth parameter represents an irrelevant rotation. Only the Jacobian

$$J = \frac{\partial(X_1', X_2')}{\partial(X_1, X_2)} = \det\begin{pmatrix} \alpha & \beta \\ \gamma & \delta \end{pmatrix} = \alpha\delta - \beta\gamma \tag{A5}$$

is important for determining the density of degeneracies. Using (A.3) and (A.4), it is easy to verify that

$$\sigma_{11}^2\sigma_{22}^2 - (\sigma_{12}^2)^2 = J^2. \tag{A6}$$

Hence if the density of degeneracies in the (X_1', X_2') space is $\mathcal{D}'$, then the density in the X_1, X_2 space is

$$\mathcal{D} = J\mathcal{D}' \tag{A7}$$

from which (3.16) follows.

APPENDIX B

For systems with a chaotic classical limit the variances and correlation coefficients of the matrix elements required for (3.16) can be obtained from a classical correlation function. Consider the expression for the mean value of the product of the matrix elements of two operators $\hat{A}$ and $\hat{B}$ in the adiabatic basis (i.e., the basis formed by the eigenstates of the Hamiltonian). This can be obtained as a function of the mean E and difference ΔE of the energies of the basis states,

$$\sigma_{AB}^2(E, \Delta E) = \frac{1}{n_0^2} \sum_{n\,(\neq m)} \sum_m \hat{A}_{nm}\, \hat{B}_{mn}^* \times\delta_\epsilon(E - \tfrac{1}{2}(E_n + E_m)) \times\delta_\epsilon(\Delta E - (E_n - E_m)), \tag{B1}$$

where the pseudo-δ functions $\delta_\varepsilon(x)$ are spread out over an energy range ε which is large compared to the mean level spacing but small compared to the classical energy scales of the problem. The quantity σ_{AB}^2 can be related to the relevant correlation function for the classical motion by a simple extension of an argument given by Wilkinson [26],

$$\sigma_{AB}^2(E, \Delta E) = \frac{1}{2\pi\hbar\rho\Omega} \int_{-\infty}^{\infty} dt\; C_{AB}(E, t)\; \exp(i\Delta E t/\hbar). \tag{B2}$$

Here the correlation function $C_{AB}(E, t)$ and the weight of the energy shell $\Omega(E)$ are defined by

$$C_{AB}(E, t) = \int d\mathbf{q} \int d\mathbf{p}\; A(\mathbf{q}, \mathbf{p}) \times B(\mathbf{q}'(\mathbf{q}, \mathbf{p}, t), \mathbf{p}'(\mathbf{q}, \mathbf{p}, t)) \times\delta(E - H(\mathbf{q}, \mathbf{p})) \tag{B3}$$

[where $(\mathbf{q}', \mathbf{p}')$ is the phase-space point that the point $(\mathbf{q}, \mathbf{p})$ evolves into after time t under the classical equations of motion] and

$$\Omega(E) = \int d\mathbf{q} \int d\mathbf{p}\; \delta(E - H(\mathbf{q}, \mathbf{p})). \tag{B4}$$

For computing the density of diabolical points, we require the variance of matrix elements between adjacent states: we therefore set $\Delta E = 0$ in the expressions above.

[1] J. von Neumann and E. P. Wigner, Phys. Z. **30**, 467 (1929).
[2] M. V. Berry and M. Wilkinson, Proc. R. Soc. A **392**, 15 (1984).
[3] E. Teller, J. Phys. Chem. **41**, 109 (1937).
[4] C. E. Zener, Proc. R. Soc. London Ser. A **137**, 696 (1932).
[5] G. Herzberg and H. C. Longuet-Higgins, Discuss. Faraday Soc. **35**, 77 (1963).
[6] D. L. Hill and J. A. Wheeler, Phys. Rev. **89**, 1102 (1952).
[7] M. V. Berry, in *Chaotic Behavior in Deterministic Systems*, edited by G. Iooss, R. H. G. Helleman, and R. Stora, Les Houches Lectures XXXVI (North-Holland, Amsterdam, 1983), pp. 171-271.
[8] S. A. Molcanov, Commun. Math. Phys. **78**, 429 (1981).
[9] *Statistical Properties of Spectra: Fluctuations*, edited by C. E. Porter (Academic, New York, 1965).
[10] M. Wilkinson, J. Phys. A **21**, 4021 (1988).
[11] M. Wilkinson and E. J. Austin, Phys. Rev. A **46**, 64 (1992).
[12] M. Wilkinson, J. Phys. A **22**, 2795 (1989).
[13] P. Gaspard, S. A. Rice, H. J. Mikeska, and K. Nakamura, Phys. Rev. A **42**, 4015 (1990).
[14] P. Pechukas, Phys. Rev. Lett. **51**, 943 (1983).
[15] E. J. Austin and M. Wilkinson, Nonlinearity **5**, 1137, (1992).
[16] J. Goldberg and W. Schwiezer, J. Phys. A **24**, 2785 (1991).
[17] J. Zakrzewski and M. Kuś, Phys. Rev. Lett. **67**, 2749 (1991).
[18] E. P. Wigner, Oak Ridge National Laboratory Report No. ORNL-2309, 1957 (unpublished), pp. 59–70.
[19] S. O. Rice, Bell. Sys. Tech. J. **24**, 46 (1945).
[20] M. S. Longuet-Higgins, Philos. Trans. R. Soc. London Ser. A **249**, 321 (1957).
[21] M. V. Berry, Proc. R. Soc. London Ser. A **392**, 45 (1984).
[22] B. Simon, Phys. Rev. Lett. **51**, 2167 (1983).
[23] J. M. Robbins and M. V. Berry, Proc. R. Soc. London Ser. A **436**, 631 (1992).
[24] A. Pandey, Ann. Phys. (N.Y.) **119**, 170 (1979).
[25] F. J. Dyson, J. Math. Phys. **3**, 429 (1962).
[26] M. Wilkinson, J. Phys. A **20**, 2415 (1987).